Quantifying Cartilage Contact Modulus, Tension Modulus, and Permeability With Hertzian Biphasic Creep

A. C. Moore
Department of Biomedical Engineering,
University of Delaware,
Newark, DE 19716

J. F. DeLucca
Department of Biomedical Engineering,
University of Delaware,
Newark, DE 19716

D. M. Elliott
Department of Biomedical Engineering,
University of Delaware,
Newark, DE 19716

D. L. Burris[1]
Department of Biomedical Engineering;
Department of Mechanical Engineering,
University of Delaware,
Newark, DE 19716
e-mail: dlburris@udel.edu

This paper describes a new method, based on a recent analytical model (Hertzian biphasic theory (HBT)), to simultaneously quantify cartilage contact modulus, tension modulus, and permeability. Standard Hertzian creep measurements were performed on 13 osteochondral samples from three mature bovine stifles. Each creep dataset was fit for material properties using HBT. A subset of the dataset ($N = 4$) was also fit using Oyen's method and FEBio, an open-source finite element package designed for soft tissue mechanics. The HBT method demonstrated statistically significant sensitivity to differences between cartilage from the tibial plateau and cartilage from the femoral condyle. Based on the four samples used for comparison, no statistically significant differences were detected between properties from the HBT and FEBio methods. While the finite element method is considered the gold standard for analyzing this type of contact, the expertise and time required to setup and solve can be prohibitive, especially for large datasets. The HBT method agreed quantitatively with FEBio but also offers ease of use by nonexperts, rapid solutions, and exceptional fit quality ($R^2 = 0.999 \pm 0.001$, $N = 13$).
[DOI: 10.1115/1.4032917]

Keywords: biphasic, cartilage, indentation, contact mechanics, compression

Introduction

Quantifying the material properties of cartilage, which is nonlinear, anisotropic, heterogeneous, and viscoelastic, has been historically challenging. Early studies used indentation measurements to study the elastic properties of cartilage [1–7], but two problems with this approach emerged. First, because cartilage is a thin layer attached to a stiff substrate, it is difficult to know the extent to which the underlying bone contributes to the deformation response. Second, the tissue creeps over time. Kempson et al. addressed the substrate problem by experimentally determining a layer correction factor [1,2], which Hayes et al. later solved for theoretically [8]. The time-dependence problem was initially addressed by defining different moduli at different times after loading (e.g., instantaneous modulus [7] and two-second creep modulus [2]).

McCutchen demonstrated that the time-dependence of the mechanical response was due to the exudation of interstitial fluid, which constitutes approximately 80% of the cartilage. His weeping lubrication theory explained creep and low friction of cartilage simultaneously [9,10]. Armstrong et al. and Mow et al. used linear mixture theory, a continuum mechanics-based approach, to solve for the biphasic (solid and fluid phase) response to unconfined and confined compression [11,12]. However, the simplifying assumptions that make these configurations theoretically attractive are impossible to achieve experimentally: (1) samples are not flat or parallel, (2) flow occurs between the cartilage and the impermeable boundary, and (3) removal of the cartilage from the bone fundamentally changes the collagen structure, and therefore tissue properties. In an effort to overcome some of these experimental challenges, Mak et al. developed a linear mixture theory solution to creep indentation of a porous plane-ended cylinder into a cartilage layer to enable in situ characterization of the compression modulus and permeability [13]. A follow-up paper describing the experimental procedure required to use the solution has since become the gold standard for quantifying biphasic compressive properties of cartilage [14].

The use of a plane-ended indenter was motivated by the theoretical benefits of a constant contact area. However, the edge of the plane-ended indenter is a stress concentrator. Spherical indenters, which eliminate the stress concentration and better represent physiological contacts, are experimentally favorable for quantifying material and tribological properties [15–18]. Spherical indentation of a linearly elastic half-space was first solved by Hertz [19] and later by Agbezuge and Deresiewicz for a linearly elastic biphasic half-space [20]. Oyen digitized their master curve, fit the points to an analytical function, and used that function to develop a method of quantifying Poisson's ratio, permeability, and shear modulus from Hertzian creep measurements [21].

Ling recognized the importance of mechanical nonlinearity (cartilage is much stiffer in tension than in compression) and, to the best of our knowledge, was the first to develop a nonlinear mixture model of cartilage mechanics and tribology [22]. Whereas linear mixture theories are known to underpredict interstitial pressure and the resulting stress-shielding and lubrication effects [11], Soltz and Ateshian [23] showed that a nonlinear mixture model accurately predicts the experimentally measured response, i.e., they showed that the stiff tension modulus effectively confines the tissue, thus providing the resistance against which interstitial pressure builds. The tension modulus is as important as the compression modulus and permeability to cartilage mechanics and tribology.

There are relatively few studies in which the compression modulus, tension modulus, and permeability have been determined for a single sample. Soltz and Ateshian [23] used a combination of unconfined compression, confined compression, and shear testing. Huang et al. [24] used a combination of tension testing and unconfined compression while Setton et al. [25] used a combination of tension testing and porous plane-ended indentation. In each of these studies, cartilage samples were removed from the bone and

[1]Corresponding author.

Contributed by the Tribology Division of ASME for publication in the Journal of Tribology. Manuscript received August 5, 2015; final manuscript received February 11, 2016; published online July 26, 2016. Assoc. Editor: Zhong Min Jin.

properties quantified with multiple testing modalities, each requiring significant test time. We recently described a method with which contact modulus, tension modulus, and permeability can be quantified using Hertzian indentation measurements on any osteochondral surface [26]; however, the fact that each indent represents a single data point limits the number of flow conditions that can be probed. This paper develops a creep-based method to quantify the best-fit contact modulus, tension modulus, and permeability properties for all possible flow rate conditions. The goal of this paper is to describe the method, apply it to a representative collection of cartilage samples, probe its limitations, and compare its output against the solutions from Oyen [21], a common biphasic characterization method, and FEBio, an open-source finite element package that is considered the current gold standard for soft tissue mechanics modeling [27].

Methods

Materials and Equipment. Thirteen osteochondral cores were removed from three mature bovine stifles: ten samples came from the femoral condyle and three came from the tibial plateau. Unless noted otherwise, each sample had a diameter of 12.7 mm. Samples were stored at 2 °C in 0.15 M phosphate buffered saline (PBS) and tested within 2 days of removal. The thickness of each cartilage sample was measured before the test with a calibrated optical microscope. The thickness was defined as the mean of four equally spaced measurements, which typically varied by less than 0.1 mm. The thickness values ranged from 0.89 to 2.34 mm. The custom indentation rig shown in Fig. 1 was used to perform creep indentation experiments. A single smooth and impermeable borosilicate glass sphere was used to indent each sample; the radius was $R = 3.175$ mm. After mounting the sample in the indenter, a two-axis tilt stage was used to orient the sample normally with respect to the loading Z-axis; an X–Y translation stage was then used to locate the sample under the indenter. The sample was then submerged in PBS for the duration of the test. For repeat testing, the sample was left submerged for 20 mins to equilibrate before subsequent testing.

A displacement controlled piezoelectric stage (Physik Instrumente P-628, 0–800 ± 0.0018 μm) was used to control each indentation. A custom load cell consisted of a calibrated cantilevered beam (0.926 ± 0.0012 mN/μm) and a capacitance sensor (0–150 ± 0.014 μm) used to measure beam deflection. The contact force was calculated by multiplying the beam deflection by the spring constant. The indentation depth of the sphere into cartilage was calculated as the difference between the stage displacement and the beam deflection.

Two tests were used: (1) creep and (2) creep relaxation. The creep test, which is used as the standard given its prevalence in the literature, applies a constant force. A custom LABVIEW program was written to achieve load control by updating the Z-stage position based on the difference between the target load and the measured load. Creep relaxation was used to: (1) demonstrate generality of the results for different testing modalities and (2) to provide an experimentally simpler alternative to constant load testing. For creep relaxation, an open-loop voltage was applied to the stage. In this case, the load decreases as the sample deforms with a ratio equal to the spring constant of the loading beam.

Prior to each indentation test, the vertical stage approached the surface until the measured force exceeded zero by three times the standard error. The probe was then retracted 3 μm above the surface before driving the probe into the sample to achieve the target load; the target load was reached within 0.7 s for each measurement. Equilibration was defined when the indentation rate fell below 0.3 μm/min, which corresponds to less than 5 Pa/min for the samples in this study [18,28].

HBT Method. The method implemented here was based on the analytical model from Moore and Burris [29], which we refer to as HBT. The model assumes: no adhesion, isotropic, homogeneous, linearly elasticity in compression, linearly elasticity in tension (different compression and tension moduli), a Poisson's ratio of zero, and biphasic with strain-dependent permeability. The first advantage to this method is that it provides an analytical framework for estimating properties.

At equilibrium, interstitial fluid pressure falls to zero and the indentation depth is only a function of the effective contact modulus ($E_{c'}$). The effective contact modulus can be determined directly from Hertz's theory using the equilibrium indentation depth

$$E_{c'} = \frac{3}{4} F \cdot R^{-0.5} \cdot \delta_{\text{eq}}^{-1.5} \tag{1}$$

where δ_{eq} is the indentation depth at equilibrium, R is the radius of the indenter, and F is the applied force. Because Eq. (1) assumes a semi-infinite half-space, the "effective" contact modulus includes contributions from the substrate. The corrected contact modulus (E_c) of the cartilage is a function of $E_{c'}$, R, δ_{eq}, and cartilage thickness, t [30]

$$E_c = E_{c'} \cdot \left(1 - 1.04 \cdot e^{\left(-1.73 \cdot \left(\frac{t}{\sqrt{R \cdot \delta_{\text{eq}}}}\right)^{0.734}\right)}\right)^3 \tag{2}$$

The initial indentation depth only depends on the contact and tension moduli; therefore, the tension modulus (E_{y+}) can be determined directly from the initial indentation depth

$$E_{y+} = \frac{3}{4} F \cdot R^{-0.5} \cdot \delta_{\text{init}}^{-1.5} - E_c \tag{3}$$

where the subscript init denotes the initial response to an instantaneously applied load.

Lai et al. showed that the intrinsic permeability (k) is not a material property; it is a function of tissue dilatation according to the function: $k = k_0 \cdot e^{-M \cdot \varepsilon}$ [31,32], where ε is the trace of the strain tensor, k_0 is the unstrained permeability constant, and M is the nonlinear flow-limiting constant. Because fluid cannot flow instantaneously, the volume change is zero initially and k_0 can be determined using the initial deformation rate ($\dot{\delta}$) and indentation depth

$$k_0 = \frac{4}{3} \frac{(R \cdot \delta_{\text{init}})^{1.5}}{F - 4/3 \cdot E_c \cdot R^{0.5} \cdot \delta_{\text{init}}^{1.5}} \cdot \dot{\delta}_{\text{init}} \tag{4}$$

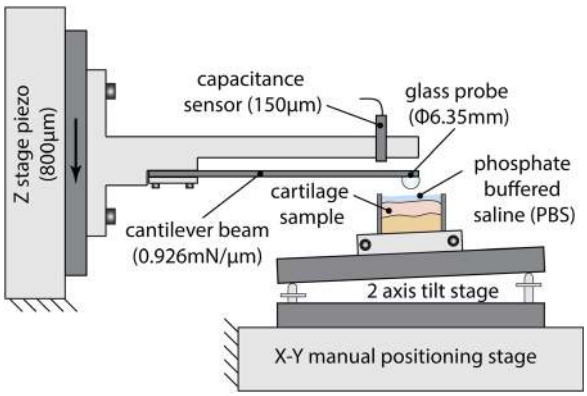

Fig. 1 Spherical indentation rig. A capacitance sensor measures beam deflection, which is proportional to force through the spring constant. As the cartilage exudes fluid and deforms the *Z*-stage piezo-actuates to maintain a constant load.

The intrinsic permeability can be determined analytically by replacing initial conditions in Eq. (4) with those at any other point; thus, M can also be determined analytically. However, a least squares regression is performed to determine the best-fit to the entire dataset. A downloadable template and user guide for the HBT method are available at the website,[2] to help other researchers obtain material properties after inserting experimental creep data.

Uncertainty analyses were performed to quantify the propagation of individual measurement uncertainties into each measured property [33]. The input measurement uncertainties were: $u(\text{time}) = 0.3$ s, $u(F) = 0.5$ mN, $u(\delta) = 1\ \mu$m, $u(R) = 3\ \mu$m, and $u(t) = 100\ \mu$m. Because the method involves numerical optimization, Monte Carlo simulations were performed to simulate the propagation of error. The Monte Carlo procedure involved: (1) perturbing the measured data by a random amount based on the appropriate uncertainties and (2) using 20 random simulated datasets with the HBT method to determine 20 unique combinations of material properties. The uncertainty in our reported measurements represents the standard deviation from those simulations.

Finally, it is important to point out some inherent limitations of the model. The anisotropic and heterogeneous nature of cartilage means that the properties depend on the material volume probed in the measurement. The Hertzian contact confines the stress field (primarily) to a hemispherical volume of the same radius as the contact; this fact provides a degree of control over the zones of the cartilage probed (e.g., the superficial zone extends from the surface to approximately 100 μm below the surface and is structurally distinct from the middle and deep zones). In addition, the flow model assumes semicircular flow streamlines, which theoretically holds as long as the contact radius is less than the cartilage thickness and half the radius of the cylindrical sample.

Comparison Studies. A subset of the measurements was fit with two accepted biphasic creep models to determine if they extract different properties from the same datasets. The first, FEBio, is an open-source finite element software package for computational tissue mechanics studies [27]. FEBio has been validated against several closed-form solutions and is considered the gold standard for the purposes of this study. FEBio was used to solve for the contact between a rigid sphere and a tension–compression nonlinear biphasic layer of cartilage bonded to a rigid substrate. The constitutive relationship assumed for articular cartilage consists of a neo-Hookean ground matrix reinforced with a spherical fiber distribution [34,35]. The FEBio algorithm adjusted compressive modulus ($E_{y-} = E_c$), fiber modulus (ξ), and permeability (k) to minimize the sum-squared error between the finite element-calculated force and the experimental force at each time step.

The second is Oyen's method, another established method of characterizing biphasic properties from Hertzian creep measurements; the method is described in detail elsewhere [21]. The method assumes linear elasticity, constant permeability, and a semi-infinite layer; we correct for the substrate effect here using Eq. (2). The Oyen method outputs contact modulus, permeability, and Poisson's ratio. A template for this procedure can be found on a separate tab of the HBT template.

The three methods (HBT, FEBio, and Oyen) provide different outputs; only the contact modulus is common among them. To compare methods, outputs were transformed into comparable parameters. The FEBio and Oyen methods provide a single effective permeability based on the best curve fit. To provide a consistent measure of permeability from HBT, a second fit is performed in which the permeability is assumed constant (i.e., M is set to zero); this has no effect on the elastic constants E_c and E_{y+}. The Oyen method assumes linear elasticity; as a result, the tensile modulus is set equal to the contact modulus. Since the FEBio method solves for the fiber modulus ξ, the tension modulus is taken as the slope of the stress–strain curve at 0% strain in a simulated tensile test using the optimized material properties from indentation.

Solutions were obtained for all three methods using each of four independent creep tests. Paired t-tests were conducted to determine whether E_c, E_{y+}, and k from HBT and Oyen methods were statistically different from those of FEBio with $p < 0.05$.

Results

HBT Method and Limitations. Three repeat creep curves are shown in Fig. 2(*a*) to illustrate a representative creep response and the extent to which that creep response is reproducible. The line represents the best-fit from HBT for curve #1 a (the worst fit of the three) and clearly represents the dataset well with $R^2 = 0.9995$. The means and standard deviations from these repeat measurements, which are shown in Fig. 2(*b*), were: $E_c = 0.59 \pm 0.01$ MPa, $E_{y+} = 7.8 \pm 0.2$ MPa, $M = 7.4 \pm 1.1$, and $k_0 = 2.20 \pm 0.24 \times 10^{-3}$ mm^4/Ns. The experimental uncertainties were: $u(E_c) = 0.02$ MPa, $u(E_{y+}) = 0.3$ MPa, $u(M) = 0.3$, and $u(k_0) = 0.06 \times 10^{-3}$ mm^4/Ns; the fact that the standard deviations were consistent with the accompanying experimental uncertainties suggests that the scatter in repeat measurements was driven at least as much by measurement uncertainty as they are by changes in the response of the cartilage itself. This demonstrates that the response is a consistent function of material constants regardless of the extent to which interstitial fluid is lost during each creep test.

In theory, the flow model is valid until the contact radius exceeds the thickness or half the sample radius. Additional indents were performed to test for these effects. Figure 3(*a*) illustrates the effect of creep load (35, 50, and 120 mN) on material properties. Increased loads sampled increased depths, which tended to increase E_c and E_{y+} and decrease k_0; these changes are consistent with known depth dependences of cartilage [36,37]. The increase in E_c reflects increased solid content in the deeper zones [36,37], while the increase in E_{y+} reflects the fact that tensile modulus increases with increased tensile strain due to fiber uncrimping [37]. The contact radius never exceeded 55% of the thickness so apparent changes in permeability with load most likely reflect actual differences between the effective depths sampled [36,37].

To evaluate the potential effects of sample size on the infinite biphasic layer assumption, a third sample was tested after trimming from Ø 19 → 12.7 → 6.35 → 4.8 mm; the results are shown in Fig. 3(*b*). Unlike the variable load test, this test effectively eliminates the confounding effect of variable sampling depth. As Fig. 3(*b*) demonstrates, the method was insensitive to variations in sample size down to 3.5× the contact diameter.

A third test of method generality was conducted by comparing results from two different loading cases: creep and creep relaxation. As Fig. 4 illustrates, the creep relaxation simultaneously involves creep and stress relaxation. There are several noteworthy features. First, the predictability (R^2) of the HBT method is equally good for both tests. Second, the material constants are insensitive to the experimental method. The permeability decreased by nearly 50% in creep relaxation, which is consistent with the fact that a higher initial load probes a deeper zone with lower permeability (consistent with Fig. 3(*a*)). Whereas the properties clearly depend on the volume being sampled, these results suggest that the HBT method is insensitive to the nature of the test itself.

Finally, measurements were performed on two different populations of cartilage: one from the tibial plateau and the other from the femoral condyle to test for sensitivity to differences between populations. The results of these measurements are shown in Fig. 5. The mean and standard deviation in the coefficient of determination for all 13 fits was $R^2 = 0.999 \pm 0.001$, which demonstrates that all samples were well fit by the method, despite obvious differences between sample populations [38]. On visual inspection, the tibial plateau appears to have smaller moduli and greater permeability, which is the expected result; interestingly,

[2] http://research.me.udel.edu/~dlburris/publicationsOther.html

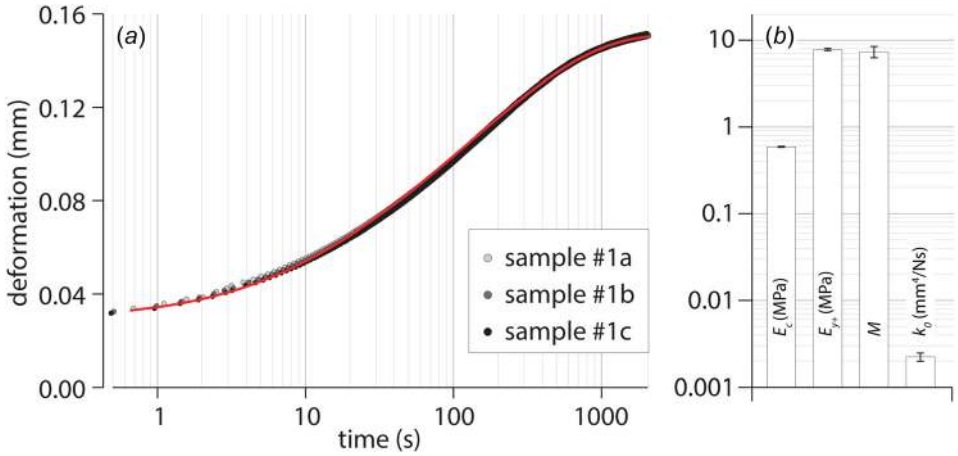

Fig. 2 (*a*) Creep deformation versus time for sample 1 at a constant load of 120 mN. Sample #1a was the first test and #1c was the last repeat; each repeat was conducted after 20 mins of free swelling. (*b*) Comparisons of E_c, E_{y+}, M, and k_0 for sample 1. Error bars represent the standard deviation of repeat measurements and fits.

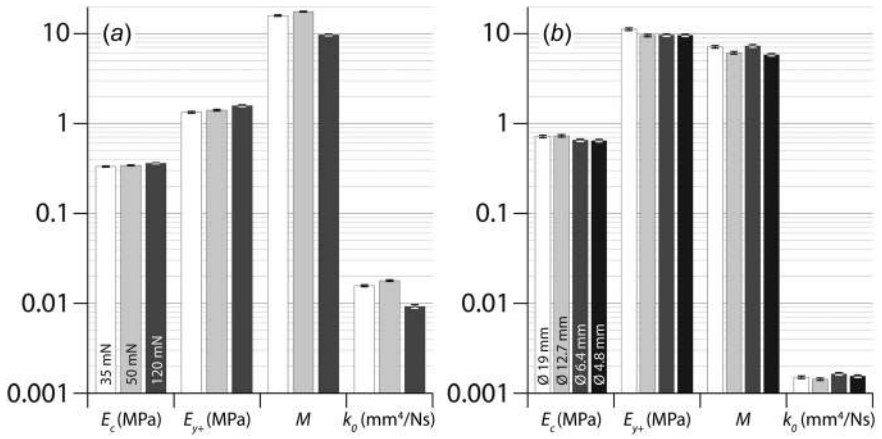

Fig. 3 Additional tests were conducted to evaluate the HBT method. (*a*) Three different creep loads (35, 50, and 120 mN) were applied to the same location on sample 2 to determine the effect of creep load on tissue properties. (*b*) Sample 3 was used to test the assumption of an infinite biphasic layer. The sample was evaluated after sequentially reducing its diameter from 19 to 4.8 mm.

there is no obvious effect of joint surface on M, which varies by less than a factor of four for all samples tested. Student t-tests detected statistically significant differences in moduli only, which is reasonable considering the relatively small sample size from the tibial plateau ($n = 3$).

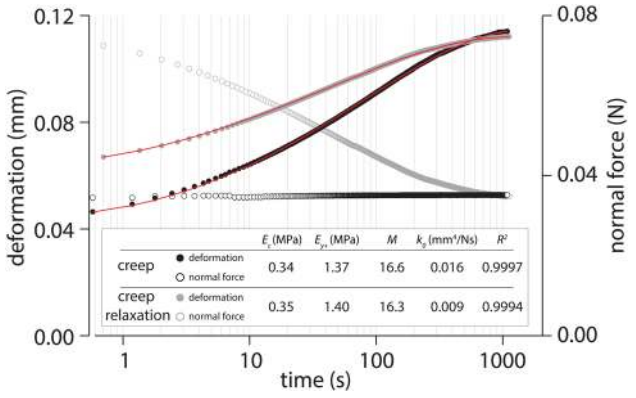

Fig. 4 Comparison of results from HBT fits to creep and creep relaxation. Creep relaxation is a hybrid of creep and stress relaxation.

Methods Comparisons. The converted values from each method are given in Table 1 for $N = 4$ samples. It is worth noting that the *effective* permeability from HBT is typically less than half k_0 due to the decrease in permeability with strain. Figure 6 compares the percent differences from the FEBio standard. The HBT method differed from FEBio by $+3\%$, $+7\%$, and -33% for E_c, E_{y+}, and k, respectively. The Oyen method differed from FEBio by -11%, -88%, and -37% for E_c, E_{y+}, and k, respectively. Differences in both moduli from the Oyen method were statistically significant; no differences were detected between HBT and FEBio.

Discussion

This study developed and illustrated a simple method of determining the contact modulus, tension modulus, and permeability properties of cartilage using a single Hertzian creep test. The key questions are whether or not the creep response is actually a function of material constants and whether or not the material constants from the model reflect actual constants of the tissue. The results of this study help build the case that the creep response does reflect material constants and that the values output by HBT reflect actual values based on direct comparisons against the finite element method and indirect comparisons against values reported in the literature.

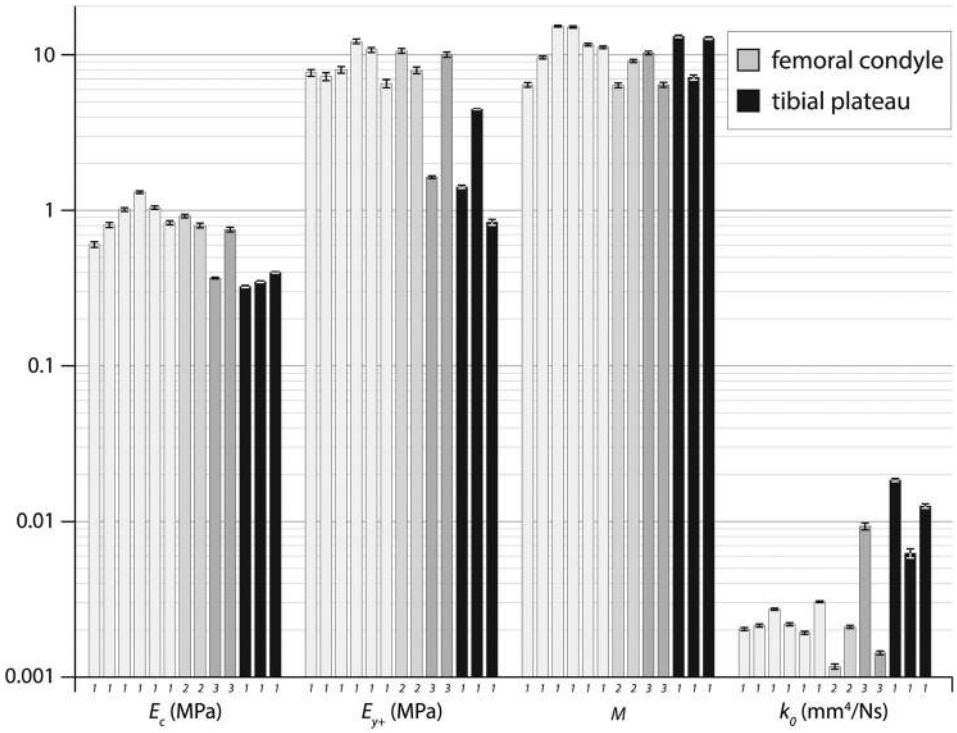

Fig. 5 Material properties for 13 samples from three bovine stifles as determined by HBT. Samples are grouped by their respective cartilage surface, femoral surface (light gray), or tibial surface (dark gray). Tibial samples were only obtained from joint 1. Femoral surfaces from different joints (1, 2, and 3) are shaded differently to highlight their differences. Error bars represent experimental uncertainty.

First, the creep response was repeatable in three subsequent measurements, which suggest that it is a function of material constants independent of the fact that previous experiments cause significant exudation of the interstitial fluid. Thus, the method can be used to determine the material constants directly prior to tribological testing, for example.

Second, the properties output by the method were independent of variations in applied load, sample size, and test configuration (creep versus creep relaxation) when the contact radius was less than 55% the cartilage thickness and less than 28% the radius of the cylindrical plug. In cases for which the interaction depth did change (variable load and creep relaxation), the stiffness increased and permeability decreased as expected based on known changes in structure and properties with depth [36,37].

Third, the HBT method fit to each dataset well regardless of the test configuration (creep versus creep relaxation) and sample population tested (femoral versus tibial); the coefficient of determination for the 13 sample dataset was $R^2 = 0.9990 \pm 0.001$. The fact that the tibial plateau tended to be softer and more permeable than the femoral condyle is also consistent with the published literature [38].

Fourth, direct comparison against FEBio revealed no statistically significant differences. On average, the HBT method differed from FEBio by +3%, +7%, and −33% for E_c, E_{y+}, and k, respectively. Although none of the differences were statistically significant, the variations in effective permeability do stand out. However, these differences appear less significant when considered in the context of strain-dependent permeability. For example, the intrinsic permeability of the sample from Fig. 2(*a*) decreased from 2.0×10^{-3} mm^4/Ns during initial contact to 0.5×10^{-3} mm^4/Ns at the end of the test. The 33% mean difference in effective permeability between FEBio and HBT is actually relatively small compared to the 300% variation in intrinsic permeability that was typical of these experiments.

Table 1 Converted values of E_c, E_{y+}, and k from the FEBio, HBT, and Oyen methods

Method	E_c (MPa)	E_{y+} (MPa)	$k \times 10^{-3}$ (mm^4/Ns)
FEBio	0.73 ± 0.39	6.5 ± 3.6	2.2 ± 2.3
HBT	0.76 ± 0.41	7.1 ± 4.4	1.0 ± 0.8
Oyen	0.66 ± 0.36	0.7 ± 0.4	1.4 ± 1.8

Values are given as the mean ± standard deviation for $N = 4$ samples.

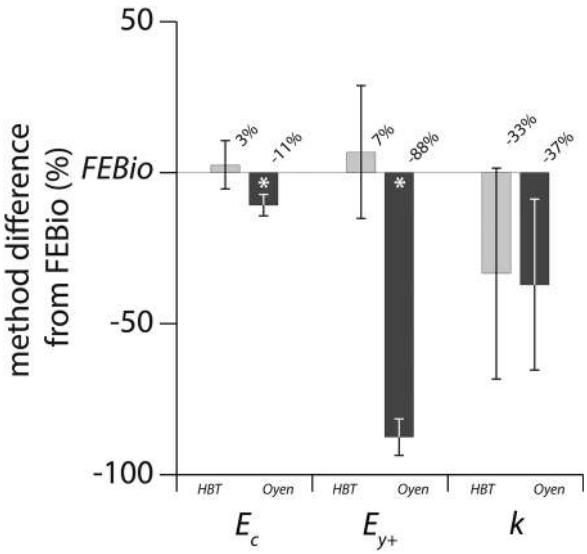

Fig. 6 The percentage difference between FEBio and the HBT (light gray) and Oyen (dark gray) methods. Error bars represent the standard deviation for $N = 4$. Asterisks (*) represent significant differences from FEBio.

Fifth, these large variations in intrinsic permeability are supported by the literature. The best resource for this analysis comes from Mow et al. [12], who directly measured intrinsic permeability under controlled external pressures and prestrains. For sample 1 (Fig. 2(*a*)), the peak interstitial pressure decreased from ~0.35 MPa to ~0 MPa and the effective strain increased from ~0.05 to ~0.2 during the creep test. Based on their results [12], this change in pressure corresponds to a ~65% reduction in permeability from 2.0 to 0.7×10^{-3} mm^4/Ns, while the change in strain corresponds to an additional ~35% reduction, bringing the intrinsic permeability to 0.5×10^{-3} mm^4/Ns. It is purely coincidental that our intrinsic permeability values perfectly match those of the sample in their study; nonetheless, their results provide direct experimental evidence that typical cartilage is expected to exhibit approximately fourfold reductions in intrinsic permeability under the conditions of these measurements. In this light, a single effective permeability analysis of creep and stress relaxation curves can be misleading, especially given that they largely reflect conditions of large strain and small pressure while physiological conditions typically involve small strains (~5% [39]) and large pressures (1–5 MPa [40]); we expect intrinsic permeability values in the joint to be close to k_0 (or a factor of ~2–3 larger than the effective permeability from a typical creep or stress relaxation experiment).

Finally, the reported values from HBT and FEBio are consistent with those of direct measurements from the literature (consistency with the Oyen method is limited to contact modulus and permeability). The tension modulus of articular cartilage is reported to range from 3.5 to 14 MPa [23,41–43]. The samples in this study had means and standard deviations of: $E_{y+} = 6.5 \pm 3.6$, 7.1 ± 4.4, and 0.7 ± 0.4 MPa, using FEBio, HBT, and Oyen fitting methods, respectively. The results from FEBio and HBT were consistent with those from the literature; the fact that they tended to fall on the lower half of the spectrum likely reflects the fact that tensile strains were small and the measurements effectively sampled closer to the toe region of the stress–strain curve. The Oyen method is unable to output a meaningful measurement of the tension modulus due to the assumption of linear elasticity. Effective permeability values for cartilage from the literature range from $k = 0.4$ to 3.6×10^{-3} mm^4/Ns [23,26,29,38,44]. The means and standard deviations from FEBio, HBT, and Oyen were: $k = 2.2 \pm 2.3$, 1.0 ± 0.8, and $1.4 \pm 1.8 \times 10^{-3}$ mm^4/Ns, respectively. In each case, the effective permeability was consistent with the previously reported results. Finally, aggregate moduli in the literature range from $H_a = 0.47$ to 0.90 MPa for a variety of joints, species, and methods [23,26,29,38,44]. The contact moduli in this study from FEBio, HBT, and Oyen were $E_c = 0.73 \pm 0.39$, 0.76 ± 0.41, and 0.66 ± 0.36 MPa, respectively, and are consistent with the compression and aggregate modulus measurements reported in the literature (all three moduli are equal if Poisson's ratio is zero [23,45,46] and if fiber tension has no significant effect on the contact modulus at equilibrium).

Conclusions

This paper develops and validates the HBT method of quantifying contact modulus, tension modulus, and permeability from Hertzian creep indentation. The method was demonstrated using creep measurements from 13 independent mature bovine cartilage samples. The results of repeat testing showed that the measured creep response is a repeatable function of material constants. In addition, any small changes in properties from variable creep loads and loading profiles were consistent with the expected effects of changes in the sampling depth. The HBT method fit experimental data well ($R^2 = 0.9988 \pm 0.0011$), detected expected differences between the tibial plateau and femoral condyle, and agreed quantitatively with FEBio, the gold standard for comparison. Both HBT and FEBio produced properties that were consistent with values in the literature obtained via more direct means. The strain-dependent permeability properties from HBT also agree well with those previously published through direct means. The analysis of the results builds a strong case in favor of the HBT method, which possesses notable advantages of experimental utility, time required, model fit quality, and consistency with prior literature.

Acknowledgment

The authors acknowledge the financial support from NIH (Grant No. P20-RR016458) for the development of the experimental and theoretical methods described in the paper. The authors also thank N.D. Garabedian for assistance in validating the Oyen method.

References

[1] Kempson, G. E., Swanson, S. A. V., Spivey, C. J., and Freeman, M. A. R., 1971, "Patterns of Cartilage Stiffness on Normal and Degenerate Human Femoral Heads," J. Biomech., **4**(6), pp. 597–609.
[2] Kempson, G. E., Freeman, M. A. R., and Swanson, S. A. V., 1971, "Determination of a Creep Modulus for Articular Cartilage From Indentation Tests on Human Femoral Head," J. Biomech., **4**(4), pp. 239–250.
[3] Parsons, J. R., and Black, J., 1977, "Viscoelastic Shear Behavior of Normal Rabbit Articular-Cartilage," J. Biomech., **10**(1), pp. 21–29.
[4] Elmore, S. M., Carmeci, P., Norris, G., and Sokoloff, L., 1963, "Nature of Imperfect Elasticity of Articular Cartilage," J. Appl. Physiol., **18**(2), pp. 393–396.
[5] Hori, R. Y., and Mockros, L. F., 1976, "Indentation Tests of Human Articular-Cartilage," J. Biomech., **9**(4), pp. 259–268.
[6] Coletti, J. M., Woo, S. L. Y., and Akeson, W. H., 1972, "Comparison of the Physical Behavior of Normal Articular Cartilage and the Arthroplasty Surface," J. Bone Jt. Surg., Am., **54**(1), pp. 147–160.
[7] Sokoloff, L., 1966, "Elasticity of Aging Cartilage," Fed. Proc., **25**(3), pp. 1089–1095.
[8] Hayes, W. C., Herrmann, G., Mockros, L. F., and Keer, L. M., 1972, "Mathematical-Analysis for Indentation Tests of Articular-Cartilage," J. Biomech., **5**(5), pp. 541–551.
[9] McCutchen, C. W., 1962, "The Frictional Properties of Animal Joints," Wear, **5**(1), pp. 1–17.
[10] McCutchen, C. W., 1959, "Sponge-Hydrostatic and Weeping Bearings," Nature, **184**(4695), pp. 1284–1285.
[11] Armstrong, C. G., Lai, W. M., and Mow, V. C., 1984, "An Analysis of the Unconfined Compression of Articular-Cartilage," ASME J. Biomech. Eng., **106**(2), pp. 165–173.
[12] Mow, V. C., Kuei, S. C., Lai, W. M., and Armstrong, C. G., 1980, "Biphasic Creep and Stress-Relaxation of Articular-Cartilage in Compression—Theory and Experiments," ASME J. Biomech. Eng., **102**(1), pp. 73–84.
[13] Mak, A. F., Lai, W. M., and Mow, V. C., 1987, "Biphasic Indentation of Articular-Cartilage.1. Theoretical-Analysis," J. Biomech., **20**(7), pp. 703–714.
[14] Mow, V. C., Gibbs, M. C., Lai, W. M., Zhu, W. B., and Athanasiou, K. A., 1989, "Biphasic Indentation of Articular-Cartilage. 2. A Numerical Algorithm and an Experimental-Study," J. Biomech., **22**(8–9), pp. 853–861.
[15] Chan, E. P., Hu, Y. H., Johnson, P. M., Suo, Z. G., and Stafford, C. M., 2012, "Spherical Indentation Testing of Poroelastic Relaxations in Thin Hydrogel Layers," Soft Matter, **8**(5), pp. 1492–1498.
[16] Bonnevie, E. D., Baro, V. J., Wang, L. Y., and Burris, D. L., 2011, "In Situ Studies of Cartilage Microtribology: Roles of Speed and Contact Area," Tribol. Lett., **41**(1), pp. 83–95.
[17] Chen, X. M., Dunn, A. C., Sawyer, W. G., and Sarntinoranont, M., 2007, "A Biphasic Model for Micro-Indentation of a Hydrogel-Based Contact Lens," ASME J. Biomech. Eng., **129**(2), pp. 156–163.
[18] Miller, G. J., and Morgan, E. F., 2010, "Use of Microindentation to Characterize the Mechanical Properties of Articular Cartilage: Comparison of Biphasic Material Properties Across Length Scales," Osteoarthritis Cartilage, **18**(8), pp. 1051–1057.
[19] Hertz, H., 1881, "On the Contact of Elastic Solids," J. Reine Angew. Math., **92**, pp.156–171.
[20] Agbezuge, L. K., and Deresiewicz, H., 1974, "Indentation of a Consolidating Half-Space," Isr. J. Technol., **12**(5–6), pp. 322–338.
[21] Oyen, M. L., 2008, "Poroelastic Nanoindentation Responses of Hydrated Bone," J. Mater. Res., **23**(5), pp. 1307–1314.
[22] Ling, F. F., 1974, "A New Model of Articular Cartilage in Human Joints," ASME J. Lubr. Technol., **96**(3), pp. 449–454.
[23] Soltz, M. A., and Ateshian, G. A., 2000, "A Conewise Linear Elasticity Mixture Model for the Analysis of Tension-Compression Nonlinearity in Articular Cartilage," ASME J. Biomech. Eng., **122**(6), pp. 576–586.
[24] Huang, C. Y., Mow, V. C., and Ateshian, G. A., 2001, "The Role of Flow-Independent Viscoelasticity in the Biphasic Tensile and Compressive Responses of Articular Cartilage," ASME J. Biomech. Eng., **123**(5), pp. 410–417.
[25] Setton, L. A., Mow, V. C., Muller, F. J., Pita, J. C., and Howell, D. S., 1994, "Mechanical-Properties of Canine Articular-Cartilage are Significantly Altered

Following Transection of the Anterior Cruciate Ligament," J. Orthop. Res., **12**(4), pp. 451–463.
[26] Moore, A. C., Zimmerman, B. K., Chen, X., Lu, X. L., and Burris, D. L., 2015, "Experimental Characterization of Biphasic Materials Using Rate-Controlled Hertzian Indentation," Tribol. Int., **89**, pp. 2–8.
[27] Maas, S. A., Ellis, B. J., Ateshian, G. A., and Weiss, J. A., 2012, "FEBio: Finite Elements for Biomechanics," ASME J. Biomech. Eng., **134**(1), p. 011005.
[28] Williamson, A. K., Chen, A. C., and Sah, R. L., 2001, "Compressive Properties and Function-Composition Relationships of Developing Bovine Articular Cartilage," J. Orthop. Res., **19**(6), pp. 1113–1121.
[29] Moore, A. C., and Burris, D. L., 2014, "An Analytical Model to Predict Interstitial Lubrication of Cartilage in Migrating Contact Areas," J. Biomech., **47**(1), pp. 148–153.
[30] Stevanovic, M., Yovanovich, M. M., and Culham, J. R., 2001, "Modeling Contact Between Rigid Sphere and Elastic Layer Bonded to Rigid Substrate," IEEE Trans. Compon. Packag. Technol., **24**(2), pp. 207–212.
[31] Lai, W. M., and Mow, V. C., 1980, "Drag-Induced Compression of Articular-Cartilage During a Permeation Experiment," Biorheology, **17**(1–2), pp. 111–123.
[32] Holmes, M. H., and Mow, V. C., 1990, "The Nonlinear Characteristics of Soft Gels and Hydrated Connective Tissues in Ultrafiltration," J. Biomech., **23**(11), pp. 1145–1156.
[33] ISO, 1993, "Guide to the Expression of Uncertainty in Measurement (Corrected and Reprinted 1995)," International Organization for Standardization, Geneva, Switzerland.
[34] Maas, S., Rawlins, D., Weiss, J., and Ateshian, G., 2011, "FEBio Theory Manual," Musculoskeletal Research Laboratories, University of Utah, Salt Lake City, UT.
[35] Ateshian, G. A., Rajan, V., Chahine, N. O., Canal, C. E., and Hung, C. T., 2009, "Modeling the Matrix of Articular Cartilage Using a Continuous Fiber Angular Distribution Predicts Many Observed Phenomena," ASME J. Biomech. Eng., **131**(6), p. 061003.
[36] Chen, A. C., Bae, W. C., Schinagl, R. M., and Sah, R. L., 2001, "Depth- and Strain-Dependent Mechanical and Electromechanical Properties of Full-Thickness Bovine Articular Cartilage in Confined Compression," J. Biomech., **34**(1), pp. 1–12.
[37] Mow, V., and Guo, X. E., 2002, "Mechano-Electrochemical Properties of Articular Cartilage: Their Inhomogeneities and Anisotropies," Annu. Rev. Biomed. Eng., **4**(1), pp. 175–209.
[38] Moore, A. C., and Burris, D. L., 2015, "Tribological and Material Properties for Cartilage of and Throughout the Bovine Stifle: Support for the Altered Joint Kinematics Hypothesis of Osteoarthritis," Osteoarthritis Cartilage, **23**(1), pp. 161–169.
[39] Eckstein, F., Tieschky, M., Faber, S., Englmeier, K. H., and Reiser, M., 1999, "Functional Analysis of Articular Cartilage Deformation, Recovery, and Fluid Flow Following Dynamic Exercise In Vivo," Anat. Embryol., **200**(4), pp. 419–424.
[40] Brand, R. A., 2005, "Joint Contact Stress: A Reasonable Surrogate for Biological Processes?," Iowa Orthop. J., **25**, pp. 82–94.
[41] Akizuki, S., Mow, V. C., Muller, F., Pita, J. C., Howell, D. S., and Manicourt, D. H., 1986, "Tensile Properties of Human Knee-Joint Cartilage. 1. Influence of Ionic Conditions, Weight Bearing, and Fibrillation on the Tensile Modulus," J. Orthop. Res., **4**(4), pp. 379–392.
[42] Basalo, I. M., Nauck, R. L., Kelly, T. A., Nicoll, S. B., Chen, F. H., Hung, C. T., and Ateshian, G. A., 2004, "Cartilage Interstitial Fluid Load Support in Unconfined Compression Following Enzymatic Digestion," ASME J. Biomech. Eng., **126**(6), pp. 779–786.
[43] Elliott, D. M., Guilak, F., Vail, T. P., Wang, J. Y., and Setton, L. A., 1999, "Tensile Properties of Articular Cartilage are Altered by Meniscectomy in a Canine Model of Osteoarthritis," J. Orthop. Res., **17**(4), pp. 503–508.
[44] Huang, C. Y., Soltz, M. A., Kopacz, M., Mow, V. C., and Ateshian, G. A., 2003, "Experimental Verification of the Roles of Intrinsic Matrix Viscoelasticity and Tension-Compression Nonlinearity in the Biphasic Response of Cartilage," ASME J. Biomech. Eng., **125**(1), pp. 84–93.
[45] Jurvelin, J. S., Buschmann, M. D., and Hunziker, E. B., 1997, "Optical and Mechanical Determination of Poisson's Ratio of Adult Bovine Humeral Articular Cartilage," J. Biomech., **30**(3), pp. 235–241.
[46] Wang, C. C. B., Chahine, N. O., Hung, C. T., and Ateshian, G. A., 2003, "Optical Determination of Anisotropic Material Properties of Bovine Articular Cartilage in Compression," J. Biomech., **36**(3), pp. 339–353.